

A CATALOG OF 120 NGC OPEN STAR CLUSTERS

A. L. Tadross

National Research Institute of Astronomy & Geophysics, Helwan, Cairo, Egypt.
email: altadross@yahoo.com

Abstract

A sample of 145 JHK–2MASS observations of NGC open star clusters is studied, of which 132 have never been studied before. Twelve are classified as non-open clusters and 13 are re-estimated self-consistently, after applying the same methods in order to compare and calibrate our reduction procedures. The fundamental and structural parameters of the 120 new open clusters studied here are derived using color-magnitude diagrams of JHK Near-IR photometry with the fitting of solar metallicity isochrones. We provide here, for the first time, a catalog of the main parameters for these 120 open clusters, namely, diameter, distance, reddening and age.

Keywords: Galaxy: open clusters and associations — individual: NGC — astrometry — Stars — astronomical databases: catalogs

1 INTRODUCTION

Systematic studies of open star clusters (OCs) are very important for understanding galactic structure and star formation processes, as well as stellar evolution and evolution of the Galactic disk. By utilizing color-magnitude diagrams (CMDs) of the stars observed in the near-infrared (NIR) bands, it is possible to determine the properties of open clusters such as distance, reddening, age and metallicity. Such parameters are necessary for studying clusters and Galactic disk. The Galactic (radial and vertical) abundance gradient also can be studied using OCs (Hou, Prantzos, & Boissier 2000; Chen, Hou, & Wang 2003; Kim & Sung 2003; Tadross 2003; Kim et al. 2005). According to some estimations, there are as many as 100,000 OCs in our Galaxy, but less than 2000 of them have been discovered and cataloged (Piskunov et al. 2006 and Glushkova et al. 2007). Actually, not all the clusters discovered so far have their basic photometrical parameters available in the current literature. However, such as yet unstudied ones are, in general, poorly populated and/or distant and/or rejected against dense foreground/background fields. In all these cases, field-star contamination is a fundamental issue that has to be dealt with before robust astrophysical parameters are derived. So, our aim in the present paper, a continuation of a series of papers, is to determine the main astrophysical properties of previously unstudied OCs using modern databases (Tadross 2008a, 2008b & Tadross 2009a, 2009b and references therein). In this respect, the present study introduces the first photometric analysis of CMDs of a sample of 120 OCs. Note that, the JHK–2MASS system gives more accurate fitting, especially for the lower portions, so that the turnoff points, distance moduli, ages and photometrical membership can be improved.

The JHK Near-IR 2MASS catalog has the advantage of being a homogeneous database, enabling us to observe young clusters in their dusty environments and reach their outer regions where low mass stars dominate. For the task of calibration, the main parameters of 13 NGC previously studied clusters are re-estimated and compared with those available in the literature. The clusters were arbitrarily selected from among the unstudied NGC candidates. The only previously known information about the investigated clusters (132 OCs) are the coordinates and the apparent diameters, which were obtained from the WEBDA¹ site and the last updated version of DIAS² collection (version 3.0, 2010 April 30). These are sorted by right ascensions and listed in Table 1 in the Appendix. The quality of the data has been taken into account and the properties of all the clusters have been estimated by applying the same method to each of them.

This paper is organized as follows. The data extraction and preparation are described in Section 2. Center determination and radial density profile are clarified in Sections 3 and 4 respectively. Sections 5, 6 and 7 are devoted to field-star decontamination, analysis of CMDs and Galactic geometric distances, respectively. The final conclusions are stated in Section. 8. All tables are reported in the Appendix.

¹<http://obswww.unige.ch/webda>

²<http://www.astro.iag.usp.br/~wilton/>

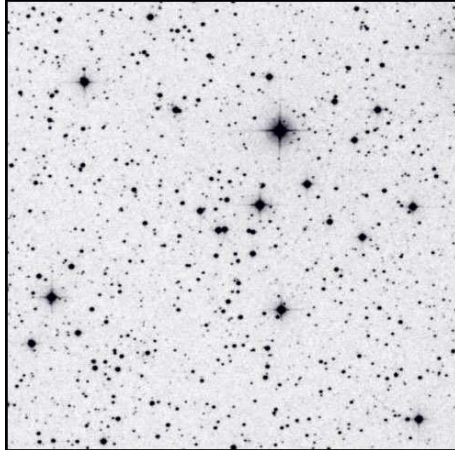


Figure 1: An example for the image of NGC 7801 as taken from DSS site. North is up, east on the left.

2 DATA EXTRACTION AND PREPARATION

The Two Micron All Sky Survey (2MASS) of Skrutskie et al. (2006) collected 25.4 T-bytes of raw imaging data covering 99.998% of the celestial sphere. Observations were conducted using two dedicated 1.3 m diameter telescopes located at Mount Hopkins, Arizona, and Cerro Tololo, Chile. 256×256 NICMOS3 (HgCdTe) arrays manufactured by Rockwell International Science Center (now Rockwell Scientific), were used which give field-of-view of $8.5' \times 8.5'$ and pixel scale of $2'' \text{ pixel}^{-1}$. The photometric system comprise J ($1.25 \mu\text{m}$), H ($1.65 \mu\text{m}$) and K_S ($2.16 \mu\text{m}$) bands, where the “ K -short” (K_S) filter excludes wavelengths longward of $2.31 \mu\text{m}$ to reduce thermal background and airglow and includes wavelengths as short as $2.00 \mu\text{m}$ to maximize bandwidth.

Data extraction has been performed using the known tool VizieR for 2MASS³ database. The investigated clusters have been selected from WEBDA and DIAS catalogues. The clusters data have been extracted at a preliminary radius of about 2 times larger than the values provided by WEBDA or/and DIAS, in circular areas centered at the coordinates of the clusters centers, covering possibly the clusters’ coronas (see Section 4). Note that, the field stars, mostly on the disk, contaminate the CMDs of low-latitude clusters, particularly at faint magnitudes and red colors. Therefore, suitable clusters should have enough members with prominent sequences in their CMDs. Further, the clusters should have good blue images on the Digitized Sky Surveys⁴ clearly separated from the background field (see the example of NGC 7801 image in Fig. 1).

A cutoff of photometric completeness limit at $J < 16.5$ mag is applied on the photometric data to avoid over-sampling (Bonatto et al. 2004). To retain the brightest stars of the cluster, the data extraction was restricted to faint stars with errors in J , H and K_S smaller than 0.2 mag. In order to establish a clean CMD for each cluster, its control field should be compared and color – magnitude filters should be applied to the cluster and its field sequences. Membership criteria is adopted for the location of the stars in the clean CMD, where the stars located away from the main sequences are excluded (Bonatto et al. 2005). The maximum departure accepted here is about 0.10 - 0.15 mag (see the example in Fig. 2).

3 CENTER DETERMINATION

To estimate the cluster center theoretically, it can be defined as either the center of mass or the location of the deepest part of the gravitational potential. Observationally, the center is often defined as the region of the highest surface brightness or the region containing the largest number of stars (Littlefair et al. 2003). Here, the cluster center is defined as the location of maximum density of probable member stars, after applying the color-magnitude filters. The optimized cluster centers can be obtained by fitting a Gaussian to the profiles of star counts, in equal incremental strips, in right ascensions and declinations. Fig. 3 represents an example for determining the cluster center of NGC 2351. All the clusters centers are found to be in agreement with our estimations within errors of a few arcseconds. Note that the coordinates of the centers of NGC 1857, NGC 2061, NGC 2234, NGC 2250 and NGC 3231 are found to be different in the WEBDA and DIAS catalogs; so we used the “Coordinate Conversion and Precession Tool” of Chandra⁵ to correct their coordinates. Meanwhile, the objects NGC 2664, NGC 5385 and NGC 6863 are demonstrated on the basis of radial

³ <http://vizier.u-strasbg.fr/viz-bin/VizieR?-source=2MASS>

⁴ <http://cadwww.dao.nrc.ca/cadcbm/getdss>

⁵ <http://cxc.harvard.edu/>

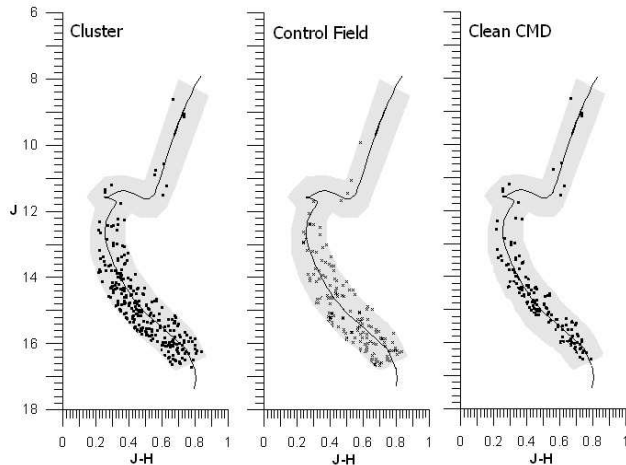


Figure 2: An example for establishing a clean CMD of NGC 7801 by comparing its control field, the dark areas represent the color and magnitude filters, which applied to the cluster and its field sequences; the maximum departure is about 0.15 mag.

velocity, original CCD photometry and proper motions to be random enhancements of field stars (Villanova et al. 2004; Moni et al. 2010).

4 RADIAL DENSITY PROFILE

The lower limit of the size of each cluster (lower border) has been obtained using the radial density profile (RDP) of the cluster’s stars. The spatial coverage and the uniformity of 2MASS photometry allows one to obtain reliable data on the projected distribution of stars over extended regions around clusters (Bonatto et al. 2005). So, within concentric shells in equal incremental steps of about $0.1 \sim 0.5$ arcmin from the cluster center, the stellar density is derived out to a pre-determined radius. Applying the empirical profile of King (1962), the cluster limiting radius can be determined at a specific point at which it reaches a stable background density. At that radius, the JHK_S photometric data would be taken into account for estimating the main cluster properties. An example for radius determination of NGC 1498 is shown in Fig. 4. On the other hand, the RDP of a cluster is used to evaluate the amount of field contamination, where the clusters of field density ≤ 2 stars per arcmin² don’t need to build the RDPs or CMDs of their fields. On the contrary, for the clusters with field density > 2 stars per arcmin², the RDPs and CMDs of their field are needed.

5 FIELD-STAR DECONTAMINATION

Usually, field stars contaminate the CMDs of a cluster, particularly at faint magnitudes and red colors. Most over-density clusters are located near the disk or/and the bulge of the Galaxy and shows crowded contaminated main sequences. These contaminated stars are always seen as a vertical redder sequence parallel to the cluster’s main sequence. CMDs of such clusters surely contain field stars that might lead to artificial isochrone solutions, i.e. one can always “fit” isochrones to such CMDs. Therefore, field-star decontamination must be used to define the intrinsic CMDs and get better isochrone fitting. To achieve this, we have to compare the CMDs of a cluster with that of a nearby control field. A control field is chosen at the same Galactic latitude, but with one degree larger or one degree smaller than that of the Galactic longitude of the cluster. From the comparison of the CMDs of such a cluster and its control field for a given magnitude and color range, we have counted the number of stars in a control field and subtracted this number from the cluster’s CMDs.

It can be noted that, for a good separated cluster, the mean density of the control field is always less than the central region of the cluster. For the sample we have investigated, we have found 12 candidates that are difficult to separate from the background field and do not have well defined RDPs or CMDs. These are NGC 1963, NGC 5269, NGC 6169, NGC 6415, NGC 6455, NGC 6476, NGC 6480, NGC 6529, NGC 6554, NGC 6682, NGC 6980, and NGC 6989. Most of them are located very close to the Galactic disk or/and in the direction of the Galactic bulge.

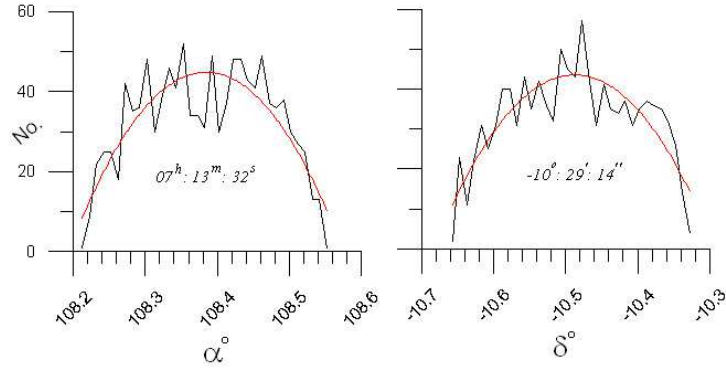


Figure 3: An example for optimizing center determination for NGC 2351, the curved lines represent the Gaussian fitting profiles. Comparing the estimated coordinates with what obtained in Table 1 in the Appendix, we found that there are differences of 1 sec in α and 2 arcsec in δ of the cluster's center.

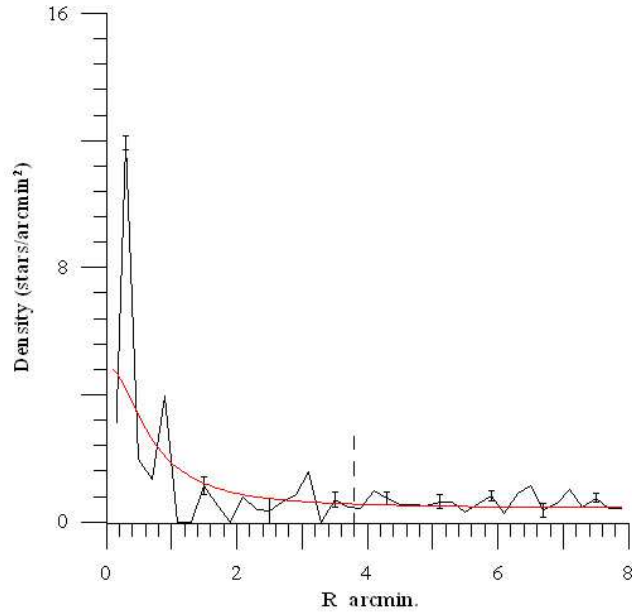


Figure 4: An example for the lower radius determination for NGC 1498, the curved line represents the fitting of King (1962) model. The length of the error bars denote errors resulting sampling statistics, in accordance with Poisson distribution. The vertical dashed line refers to that point, at which the radius determine; reaching the background density of about 0.4 stars per arcmin².

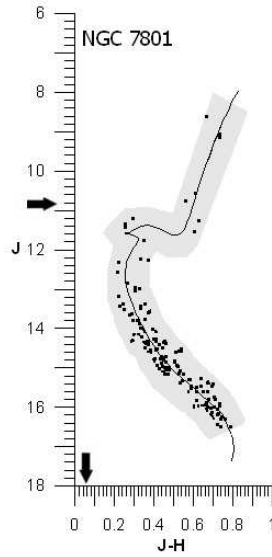


Figure 5: An example for estimating the main astrophysical parameters of NGC 7801. The age, reddening and mean distance modulus are obtained from the new theoretical Padova isochrones of solar metallicity (Bonatto et al. 2004; Bica, et al. 2006) after applying the color and magnitude filters to $J \sim (J-H)$ sequence, see Fig. 2. The age = 1.7 Gyr, $E_{J-H}=0.06$ mag, and $(m - M)_J= 10.8$ mag. The fitting errors are $\sim \pm 0.10$ mag in distance modulus, and $\sim \pm 0.05$ mag in color excess.

6 COLOR MAGNITUDE DIAGRAM ANALYSIS

CMDs are established for the stars inside radii of $1'$, $2'$, $3'$ etc. from the optimized coordinates of the centers of the clusters under investigation. We have fitted the new theoretical computed with the 2MASS J, H and K_S filters (Bonatto et al. 2004; Bica et al. 2006) to derive the cluster parameters. The simultaneous fittings were attempted on the $J \sim (J-H)$ and $K_S \sim (J-K_S)$ diagrams for the inner stars, which should be less contaminated by the background field.

If the number of stars are not enough for an accepted fitting, the next larger area is included, and so on. In this way, different isochrones of different ages have been applied on the CMDs of each cluster, fitting the lower envelope of the points matching the main sequence stars, turn-off point and red giant positions. Guiding by the Galactic reddening values of Schlegel et al. (1998), the average age and distance modulus are determined for each cluster. Although Schlegel's reddening values are often overestimated at low Galactic latitudes, it is still a useful source of data. Comparing our estimated reddening values with the reliable ones of Schlegel's, we found that 96% of our sample are in agreement with Schlegel's values within ranging errors of 0.05 mag. (see Table 3 in the Appendix). The distance modulus is taken at the proper values within a ranging fitting error of about ± 0.10 mag. Fig. 5 represents an example for estimating the main parameters of NGC 7801.

The observed data has been corrected for interstellar reddening using the coefficients ratios $\frac{A_J}{A_V} = 0.276$ and $\frac{A_H}{A_V} = 0.176$, which were derived from absorption ratios in Schlegel et al. (1998), while the ratio $\frac{A_{K_S}}{A_V} = 0.118$ was derived from Dutra et al. (2002). Therefore $\frac{E_{J-H}}{E_{B-V}} = 0.309$, $\frac{E_{J-K_S}}{E_{B-V}} = 0.488$, and then $\frac{E_{J-K_S}}{E_{J-H}} \approx 1.6 \pm 0.15$ can be derived easily from the above ratios, where $R_V = \frac{A_V}{E_{B-V}} = 3.1$.

7 GALACTIC GEOMETRIC DISTANCES

Galactic geometric distances are the distance from the sun, R_\odot , distance from the Galactic center, R_{gc} , and the projected rectangular distances on the Galactic plane centered on the Sun, X_\odot , Y_\odot , as well as the distance from Galactic plane, Z_\odot . The importance of such distances is that they can be used to investigate the geometry of the Galaxy or/and the traces of the Milky-Way arms. Fig. 6 represents a sketch-chart for the calculation of the geometric distances for a cluster in the Galaxy, taken from Tadross (2000).

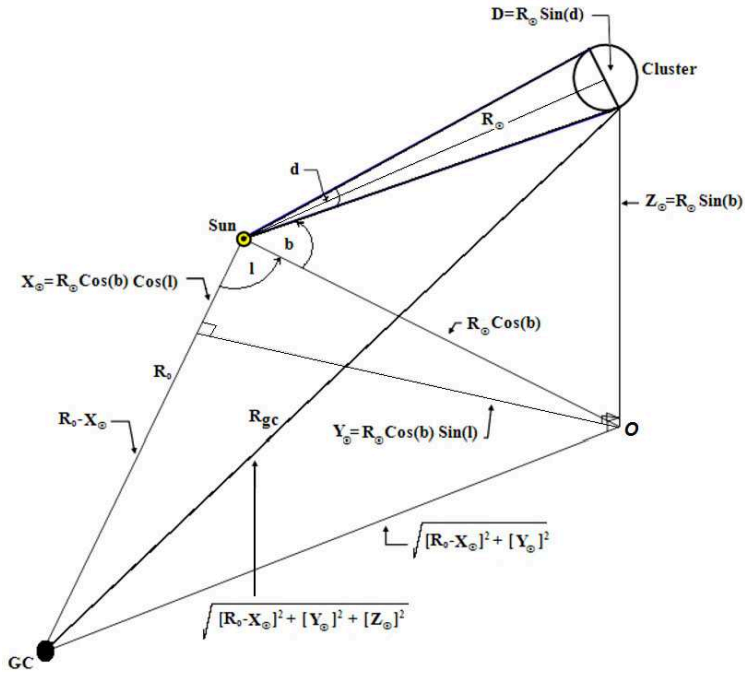


Figure 6: A sketch-chart illustrates the Galactic geometric distances for a cluster in the Galaxy; taken from Tadross, A. L. (2000). Let the cluster's distances from the sun, R_{\odot} , from the Galactic center, R_{gc} , and the horizontal projected rectangular distances on the Galactic plane centered on the Sun, X_{\odot} , Y_{\odot} , and the distance from Galactic plane, Z_{\odot} . The sun's distance from the galactic center $R_o=8.5$ kpc; d & D are the angular and linear diameter of the cluster; ℓ & b are the galactic longitude and latitude of the cluster.

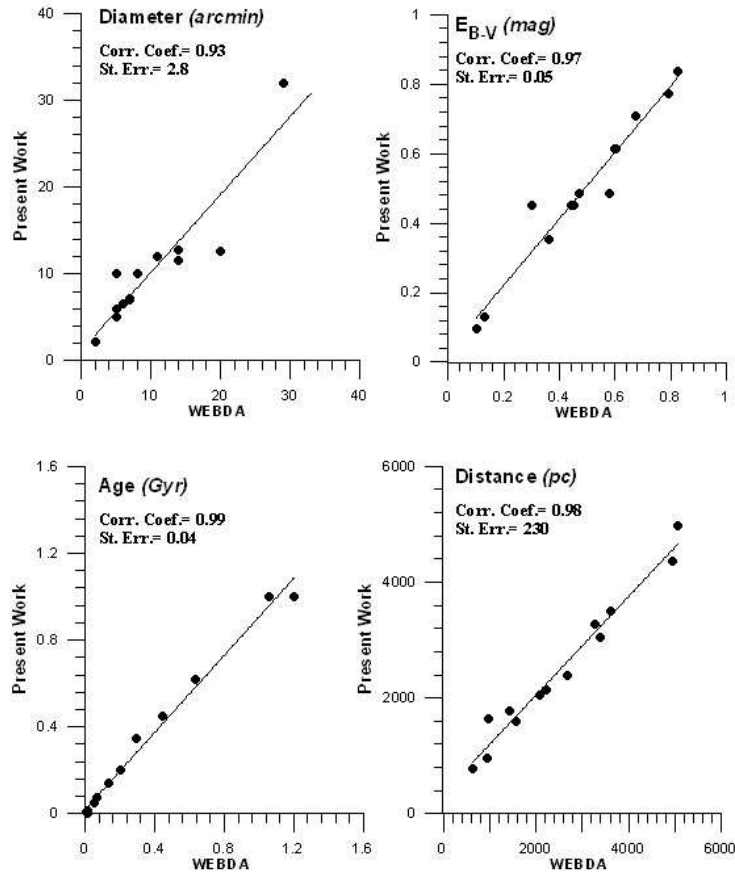


Figure 7: The comparison results of the main parameters of thirteen clusters with those in the literature. Diameters, color excesses, ages and distances with the correlation coefficient and standard error for each relation are obtained.

8 CONCLUSIONS

Following the above procedures, the basic astrophysical parameters, namely, angular diameter, age, reddening, distance modulus and the Galactic geometric distances, have been obtained for 120 NGC previously unstudied open clusters. The results may be used to investigate, for instance, the cluster formation rate, the geometry of the Galaxy, the time scale for cluster dissolution, etc. The same procedures have been applied to re-estimate 13 previously studied NGC clusters for calibration purposes. It must be mentioned that some distant clusters which lie behind or embedded within dark clouds of gas and dust are influenced by differential reddening that lead to some biases in estimating parameters from optical data. Such clusters are heavily obscured in the optical, but easily detected in the infrared band. On the other hand, it is difficult to detect the cluster members in the infrared band, especially those with low stellar density, because of the huge background field. Therefore, the difficulties in the detection and extraction of cluster members increasingly worsen towards NIR bands (Zakharova & Loktin 2006).

A Comparison of the astrophysical parameters of the thirteen clusters that overlap between the present work and those in WEBDA are listed in Table 2 in the Appendix. The relations between the present results and those obtained from WEBDA for diameter, color excess, age and distance can be seen in Fig. 7. The correlation coefficient and standard error for each relation are shown in the same figure. We can see that the derived parameters are reasonable and very close to the published ones, which indicates that our reduction procedure is very reliable. The final results of the investigated 133 star clusters that investigated here are listed in Table 3 in the Appendix. All the CMDs of our sample are electronically available on demand.

Acknowledgments

This publication makes use of data products from the Two Micron All Sky Survey *2MASS*, which is a joint project of the University of Massachusetts and the Infrared Processing and Analysis Center/California Institute of Technology, funded by the National Aeronautics and Space Administration and the National Science Foundation. Catalogues from *CDS/SIMBAD* (Strasbourg), and Digitized Sky Survey *DSS* images from the Space Telescope Science Institute have been employed.

References

- Bica, E., Bonatto, Ch., Blumberg, R. 2006, *A&A*, 460, 83
- Bonatto, Ch., Bica, E., Girardi, L. 2004, *A&A*, 415, 571
- Bonatto, Ch., Bica, E., Santos, J. 2005, *A&A*, 433, 917
- Chen, L., Hou, J., Wang, J. 2003, *AJ*, 125, 1397
- Dutra, C., Santiago, B., Bica, E. 2002, *A&A*, 381, 219
- Glushkova, E., Kopusov, S., Zolotukhin, I. 2008, *A&A*, 486, 771
- Hou, J., Prantzos, N., Boissier, S. 2000, *A&A*, 362, 921
- Kim, S., Sung, H. 2003, *JKAS*, 36, 13
- Kim, S., et al. 2005, *JKAS*, 38, 429
- King, I. 1962, *AJ*, 67, 471
- Littlfair, S. et al. 2003, *MNRAS*, 345, 1205
- Moni, C. et al. 2010, *A&A*, 510, 44
- Piskunov, A., et al. 2006, *A&A*, 445, 545
- Schlegel, D., Finkbeiner, D., Davis, M. 1998, *ApJ*, 500, 525
- Skrutskie, M., Cutri, R., Stiening, R., et al. 2006, *AJ*, 131, 1163
- Tadross, A. L. 2000, PhD thesis, Faculty of Science, Cairo University, pp. 15
- Tadross, A. L. 2003, *NewA*, 8, 737
- Tadross, A. L. 2008*a*, *NewA*, 13, 370
- Tadross, A. L. 2008*b*, *MNRAS*, 389, 285
- Tadross, A. L. 2009*a*, *NewA*, 14, 200
- Tadross, A. L. 2009*b*, *Ap&SS*, 323, 383
- Villanova, S. et al. 2004, *A&A*, 428, 67
- Zakharova, P. E., Loktin, A. V. 2006, *A&AT*, 25, 171

Table 1: The equatorial, Galactic positions and the diameters of the investigated clusters, as taken from “Webda” and “Dias”; sorted by right ascensions.

Index	Cluster	$\alpha^{\text{h m s}}$	$\delta^{\circ ' ''}$	G. Long. $^{\circ}$	G. Lat. $^{\circ}$	Diam. $'$
1	NGC 7801	00:00:21	+50:44:30	114.73	-11.315	8
2	NGC 7826	00:05:17	-20:41:30	61.875	-77.653	20
3	NGC 7833	00:06:31	+27:38:30	110.9	-34.178	1.3
4	NGC 110	00:27:25	+71:23:00	121	8.602	20
5	NGC 272	00:51:24	+35:49:54	122.93	-27.05	4
6	NGC 305	00:56:20	+12:04:00	124.83	-50.787	6
7	NGC 657	01:43:21	+55:50:11	130.22	-6.299	4
8	NGC 743	01:58:37	+60:09:18	131.2	-1.633	6
9	NGC 956	02:32:30	+44:35:36	141.18	-14.624	9
10	NGC 1520	03:57:51	-76:47:42	291.14	-35.705	5
11	NGC 1498	04:00:18	-12:00:54	203.62	-43.33	2
12	NGC 1557	04:13:11	-70:28:18	283.77	-38.261	21
13	NGC 1785	04:58:35	-68:50:40	280.01	-35.247	3
14	NGC 1724	05:03:32	+49:29:30	158.45	4.845	2
15	NGC 1807	05:10:43	+16:31:18	186.09	-13.495	15
16	NGC 1857*	05:20:12	+39:21:00	168.41	1.279	6
17	NGC 1891	05:21:25	-35:44:24	239.7	-32.878	15
18	NGC 1963 ^z	05:32:17	-36:23:30	240.99	-30.869	13
19	NGC 2017	05:39:17	-17:50:48	221.62	-23.708	6
20	NGC 2061*	05:42:42	-34:00:34	238.92	-28.231	16
21	NGC 2026	05:43:12	+20:08:00	187.23	-5.059	11
22	NGC 2039	05:44:00	+08:41:30	197.58	-10.274	30
23	NGC 2013	05:44:01	+55:47:36	156.51	13.417	4
24	NGC 2063	05:46:43	+08:46:54	197.29	-10.766	9
25	NGC 2132	05:55:18	-59:54:36	268.69	-30.2	17
26	NGC 2165	06:11:04	+51:40:36	162.16	15.13	9
27	NGC 2189	06:12:09	+01:03:54	207.46	-8.24	7
28	NGC 2220	06:21:11	-44:45:30	252.5	-23.926	13
29	NGC 2219	06:23:44	-04:40:36	213.96	-8.288	6
30	NGC 2224	06:27:28	+12:35:36	198.97	0.544	13
31	NGC 2234*	06:29:24	+16:41:00	195.61	2.812	25
32	NGC 2250*	06:32:48	-05:02:00	215.31	-6.432	3
33	NGC 2248	06:34:35	+26:18:16	187.54	8.247	1.5
34	NGC 2260	06:38:03	-01:28:24	212.72	-3.65	18
35	NGC 2265	06:41:41	+11:54:18	201.23	3.268	9
36	NGC 2312	06:58:47	+10:17:42	204.56	6.29	6
37	NGC 2318	06:59:27	-13:41:54	226.05	-4.46	12
38	NGC 2348	07:03:03	-67:24:42	278.14	-23.809	18
39	NGC 2331	07:06:59	+27:15:42	189.73	15.218	14
40	NGC 2338	07:07:47	-05:43:12	219.89	1.012	3
41	NGC 2349	07:10:48	-08:35:36	222.78	0.351	10
42	NGC 2352	07:13:05	-24:02:18	236.77	-6.263	6
43	NGC 2351	07:13:31	-10:29:12	224.77	0.068	4
44	NGC 2364	07:20:46	-07:33:00	223.0	3.02	6
45	NGC 2408	07:40:09	+71:39:18	143.63	29.466	24

Table 1. — Continued

Index	Cluster	$\alpha^h m s$	$\delta^\circ ' ''$	G. Long. $^\circ$	G. Lat. $^\circ$	Diam. $'$
46	NGC 2455	07:49:01	-21:18:06	238.35	2.32	5
47	NGC 2459	07:52:02	+09:33:24	211.11	17.762	1
48	NGC 2587	08:23:25	-29:30:30	249.46	4.472	2
49	NGC 2609	08:29:32	-61:06:36	276.15	-12.754	5
50	NGC 2666	08:49:47	+44:42:12	175.92	39.278	11
51	NGC 2678	08:50:02	+11:20:18	216.04	31.421	10
52	NGC 2932	09:35:28	-46:48:36	271.76	3.855	20
53	NGC 2995	09:44:04	-54:46:48	278.05	-1.228	4.5
54	NGC 3231*	10:26:58	+66:48:55	141.96	44.604	2.5
55	NGC 3446	10:52:12	-45:08:54	281.86	12.79	15
56	NGC 3520	11:07:08	-18:01:24	270.77	38.25	0.6
57	NGC 3909	11:49:49	-48:15:06	292.46	13.363	15
58	NGC 4230	12:17:20	-55:06:06	298.03	7.445	8
59	NGC 5155	13:29:35	-63:25:30	307.18	-0.869	12
60	NGC 5269	13:44:44	-62:54:54	308.96	-0.668	3
61	NGC 5284 ^x	13:46:41	-59:12:00	309.96	2.916	30
62	NGC 5299	13:50:26	-59:56:54	310.26	2.081	25
63	NGC 5381	14:00:41	-59:35:12	311.6	2.114	11
64	NGC 5800	15:01:47	-51:55:06	322.44	5.946	12
65	NGC 5925	15:27:26	-54:31:42	324.36	1.72	20
66	NGC 5998	15:49:34	-28:35:18	343.82	19.809	4
67	NGC 6169 ^x	16:34:04	-44:02:42	339.38	2.515	12
68	NGC 6334	17:20:49	-36:06:12	351.15	0.475	20
69	NGC 6360	17:24:27	-29:52:18	356.73	3.13	5
70	NGC 6357	17:24:43	-34:12:06	353.17	0.895	2
71	NGC 6374	17:32:18	-32:36:00	355.38	0.465	4
72	NGC 6415 ^x	17:44:18	-35:04:00	354.41	-2.753	?
73	NGC 6421	17:45:44	-33:41:36	355.9	-2.405	8
74	NGC 6437	17:48:24	-35:21:00	354.44	-4.184	15
75	NGC 6455 ^x	17:51:08	-35:20:18	355.32	-4.33	8
76	NGC 6476 ^x	17:54:02	-29:08:42	0.805	-1.704	?
77	NGC 6480 ^x	17:54:26	-30:27:06	359.7	-2.44	5
78	NGC 6525	18:02:06	+11:01:24	37.378	15.89	8
79	NGC 6529 ^x	18:05:29	-36:17:48	355.71	-7.3	16
80	NGC 6554 ^x	18:08:59	-18:26:06	11.762	0.648	20
81	NGC 6573	18:13:41	-22:07:06	9.063	-2.091	1
82	NGC 6595	18:17:04	-19:51:54	11.422	-1.713	4
83	NGC 6605	18:18:21	-14:56:42	15.9	0.35	15
84	NGC 6588	18:20:33	-63:48:30	330.84	-20.878	5
85	NGC 6659	18:33:59	+23:35:42	52.48	14.156	7
86	NGC 6682 ^x	18:39:37	-04:48:48	27.302	0.427	19
87	NGC 6698	18:48:04	-25:52:42	9.255	-10.792	10
88	NGC 6724	18:56:46	+10:25:42	42.842	3.577	3
89	NGC 6735	19:00:37	-00:28:30	34.402	-1.825	12
90	NGC 6743	19:01:20	+29:16:36	60.367	10.922	7
91	NGC 6773	19:15:03	+04:52:54	39.976	-3.003	8
92	NGC 6775	19:16:48	-00:55:24	36.657	-5.217	2

Table 1. — Continued

Index	Cluster	α ^{h m s}	δ ^{° ' "}	G. Long. [°]	G. Lat. [°]	Diam. [']
93	NGC 6795	19:26:22	+03:30:54	40.077	-6.137	8
94	NGC 6815	19:40:44	+26:45:30	62.135	2.045	30
95	NGC 6832	19:48:15	+59:25:18	92.005	16.349	15
96	NGC 6837	19:53:08	+11:41:54	50.519	-8.009	3
97	NGC 6839	19:54:33	+17:56:18	56.114	-5.152	6
98	NGC 6840	19:55:18	+12:07:36	51.162	-8.253	6
99	NGC 6843	19:56:06	+12:09:48	51.293	-8.404	5
100	NGC 6846	19:56:28	+32:20:54	68.691	1.919	2
101	NGC 6847	19:56:37	+30:12:48	66.882	0.783	30
102	NGC 6856	19:59:17	+56:07:48	89.683	13.527	2
103	NGC 6858	20:02:56	+11:15:30	51.36	-10.305	10
104	NGC 6859	20:03:49	+00:26:36	41.812	-15.836	8
105	NGC 6873	20:07:13	+21:06:06	60.451	-6.154	15
106	NGC 6895	20:16:29	+50:13:48	85.887	8.281	30
107	NGC 6904	20:21:48	+25:44:24	66.135	-6.311	8
108	NGC 6938	20:34:42	+22:12:54	64.91	-10.743	7
109	NGC 6950	20:41:04	+16:37:06	61.107	-15.198	15
110	NGC 6980 ^x	20:52:48	-05:50:12	42.105	-29.578	10
111	NGC 6989 ^x	20:54:06	+45:14:24	85.654	0.238	10
112	NGC 7023	21:01:35	+68:10:12	104.06	14.19	5
113	NGC 7011	21:01:49	+47:21:12	88.126	0.607	3
114	NGC 7005	21:01:57	-12:52:50	35.81	-34.711	1.5
115	NGC 7024	21:06:09	+41:29:18	84.265	-3.877	5
116	NGC 7037	21:10:54	+33:45:48	79.133	-9.761	6
117	NGC 7050	21:15:12	+36:10:24	81.533	-8.774	7
118	NGC 7055	21:19:30	+57:34:12	97.449	5.597	3
119	NGC 7071	21:26:39	+47:55:12	91.426	-2.024	3
120	NGC 7084	21:32:33	+17:30:30	69.963	-24.302	16
121	NGC 7093	21:34:21	+45:57:54	91.043	-4.348	9
122	NGC 7129	21:42:59	+66:06:48	105.4	9.885	7
123	NGC 7127	21:43:41	+54:37:48	97.907	1.15	5
124	NGC 7134	21:48:55	-12:58:24	41.98	-45.141	1
125	NGC 7175	21:58:46	+54:49:06	99.717	-0.075	29
126	NGC 7193	22:03:03	+10:48:06	70.094	-34.279	13
127	NGC 7352	22:39:43	+57:23:42	105.9	-1.054	5
128	NGC 7394	22:50:23	+52:08:06	104.79	-6.422	9
129	NGC 7429	22:56:00	+59:58:24	108.96	0.272	14
130	NGC 7686	23:30:07	+49:08:00	109.51	-11.608	14
131	NGC 7708	23:35:01	+72:50:00	117.4	10.788	23
132	NGC 7795	23:58:37	+60:02:06	116.38	-2.163	21

Table 2: The available parameters of the calibrated clusters as obtained from “Webda”.

Index	Cluster	$\alpha^{\text{h m s}}$	$\delta^{\circ ' ''}$	G. Long. $^{\circ}$	G. Lat. $^{\circ}$	Dist. <i>pc.</i>	E(B-V) <i>mag.</i>	Age <i>G yr.</i>	Diam. $'$ <i>arcmin.</i>
1	NGC 133	00:31:19	+63:21:00	120.678	0.566	630	0.60	0.01	7
2	NGC 1893	05:22:44	+33:24:42	173.585	-1.68	3280	0.58	0.01	11
3	NGC 2158	06:07:25	+24:05:48	186.634	1.781	5071	0.36	1.05	5
4	NGC 2266	06:43:19	+26:58:12	187.79	10.294	3400	0.10	0.63	5
5	NGC 2588	08:23:10	-32:58:30	252.28	2.449	4950	0.30	0.45	2
6	NGC 3496	10:59:36	-60:20:12	289.515	-0.411	990	0.47	0.30	8
7	NGC 6005	15:55:48	-57:26:12	325.78	-2.986	2690	0.45	1.20	5
8	NGC 6451	17:50:41	-30:12:36	359.478	-1.601	2080	0.67	0.14	7
9	NGC 6603	18:18:26	-18:24:24	12.86	-1.306	3600	0.79	0.20	6
10	NGC 6755	19:07:49	+04:16:00	38.598	-1.688	1421	0.83	0.05	14
11	NGC 6871	20:05:59	+35:46:36	72.645	2.054	1574	0.44	0.01	29
12	NGC 7039	21:10:48	+45:37:00	87.879	-1.705	951	0.13	0.07	14
13	NGC 7380	22:47:21	+58:07:54	107.141	-0.884	2222	0.60	0.01	20

Table 3: The derived astrophysical parameters for the investigated clusters. Columns display, respectively, index, cluster name, angular diameter, age, reddening, Schlegel’s et al. reddening values, distance modulus, distance from the sun, distance from the Galactic center, the projected distances on the Galactic plane from the sun, and the distance from Galactic plane.

Index	Cluster	Diam. <i>arcmin</i>	Age <i>Gyr</i>	E_{B-V} <i>mag</i>	Sch. <i>mag</i>	m-M <i>mag</i>	Dist. <i>pc</i>	R_{gc} <i>kpc</i>	X_{\odot} <i>pc</i>	Y_{\odot} <i>pc</i>	Z_{\odot} <i>pc</i>
1	NGC 7801	8.0	1.7 ± 0.12	0.17 ± 0.05	0.19	10.7 ± 0.1 \downarrow	1275 ± 60	9.11	523	1136	-250
2	NGC 7826	20.0	2.2 ± 0.09	0.03 ± 0.01	0.02	9.00	620 ± 29	8.23	-62	117	-606
3	NGC 7833	2.6	2.0 ± 0.08	0.06 ± 0.02	0.07	10.8	1410 ± 65	9.10	416	1090	-792
4	NGC 110	22.0	0.9 ± 0.04	0.46 ± 0.10	0.44	10.7	1150 ± 53	9.14	585	975	172
5	NGC 133 ^c	7.0	0.01 ± 0.00	0.61 ± 0.10	1.45 \dagger	10.0	780 ± 36	8.92	398	671	8
6	NGC 272	6.4	2.5 ± 0.10	0.06 ± 0.02	0.05	10.2	1068 ± 50	9.12	517	798	-486
7	NGC 305	7.0	2.0 ± 0.08	0.06 ± 0.02	0.07	10.9	1475 ± 68	9.42	533	765	-1143
8	NGC 657	6.0	1.6 ± 0.11	0.34 ± 0.05	0.36	11.0	1372 ± 63	9.44	881	1041	-151
9	NGC 743	8.0	0.5 ± 0.02	0.95 ± 0.20	0.96	11.9	1618 ± 75	9.64	1065	1217	-46
10	NGC 956	10.0	1.0 ± 0.04	0.10 ± 0.05	0.09	10.9	1455 ± 67	9.68	1097	883	-367
11	NGC 1520	7.2	2.0 ± 0.08	0.06 ± 0.01	0.08	9.50	775 ± 36	8.25	-227	-587	-452
12	NGC 1498	7.6	1.6 ± 0.11	0.04 ± 0.02	0.05	10.1	1020 ± 47	9.44	680	-297	-700
13	NGC 1557	26.0	3.0 ± 0.12	0.11 ± 0.05	0.10	10.2	1055 ± 49	8.31	-197	-805	-653
14	NGC 1785	6.0	0.5 ± 0.02	0.06 ± 0.02	0.08	12.5	3080 ± 140	8.52	-437	-2477	-1777
15	NGC 1724	16.0	0.6 ± 0.02	0.57 ± 0.10	0.58	11.3	1437 ± 66	9.85	1332	526	121
16	NGC 1807	18.0	1.0 ± 0.04	0.32 ± 0.05	0.30	10.2	960 ± 44	9.46	928	-99	-224
17	NGC 1857	8.0	0.16 ± 0.12	0.97 ± 0.20	0.99	11.8	1545 ± 71	10.02	1513	310	34
18	NGC 1891	20.0	2.0 ± 0.05	0.03 ± 0.02	0.04	9.70	860 ± 40	8.96	364	-624	-467
19	NGC 1893 ^c	12.0	0.005 ± 0.00	0.48 ± 0.05	2.13 \dagger	13.0	3270 ± 150	11.75	3248	365	-95
20	NGC 2017	12.0	1.6 ± 0.11	0.06 ± 0.02	0.06	10.3	1120 ± 52	9.37	767	-681	-450
21	NGC 2061	18.0	2.1 ± 0.08	0.03 ± 0.01	0.04	8.70	542 ± 25	8.79	246	-409	-256
22	NGC 2026	16.0	0.55 ± 0.02	0.60 ± 0.10	0.59	11.3	1418 ± 65	9.91	1401	-178	-125
23	NGC 2039	10.0	1.2 ± 0.05	0.32 ± 0.05	0.33	10.1	920 ± 42	9.38	863	-273	-164
24	NGC 2013	6.0	1.5 ± 0.06	0.23 ± 0.05	0.21	10.4	1100 ± 51	9.52	981	426	255
25	NGC 2063	12.0	1.3 ± 0.05	0.32 ± 0.05	0.33	11.2	1525 ± 70	9.97	1430	-445	-285
26	NGC 2132	24.0	1.65 ± 0.12	0.06 ± 0.02	0.05	10.0	974 ± 45	8.58	19	-842	-490
27	NGC 2158 ^c	10.0	1.00 ± 0.04	0.35 ± 0.02	0.79	13.8	4980 ± 230	13.46	4944	-575	155
28	NGC 2165	10.0	1.5 ± 0.06	0.23 ± 0.05	0.23	11.0	1445 ± 67	9.89	1328	427	377
29	NGC 2189	14.0	0.8 ± 0.03	0.39 ± 0.05	0.37	11.7	1869 ± 86	10.19	1641	-853	-268
30	NGC 2220	13.0	3.0 ± 0.12	0.06 ± 0.01	0.06	10.4	1170 ± 54	8.92	322	-1020	-475
31	NGC 2219	7.0	0.8 ± 0.03	0.40 ± 0.08	0.41	11.9	2023 ± 93	10.24	1660	-1118	-292
32	NGC 2224	14.0	0.01 ± 0.00	1.00 ± 0.25	0.99	12.8	2415 ± 111	10.81	2284	-785	23
33	NGC 2234	28.0	0.8 ± 0.03	0.51 ± 0.10	0.53	11.5	1617 ± 75	10.07	1555	-434	79
34	NGC 2250	4.0	0.6 ± 0.02	0.48 ± 0.10	0.49	11.7	1795 ± 83	10.02	1456	-1031	-201
35	NGC 2248	3.0	1.0 ± 0.04	0.23 ± 0.05	0.22	11.4	1740 ± 80	10.23	1707	-226	250
36	NGC 2260	20.0	0.01 ± 0.00	1.25 ± 0.20	1.26	12.6	1985 ± 90	10.23	1667	-1071	-126
37	NGC 2265	12.0	0.3 ± 0.01	0.48 ± 0.10	0.48	12.1	2160 ± 100	10.54	2010	-781	123
38	NGC 2266 ^c	5.0	0.62 ± 0.02	0.10 ± 0.05	0.11	12.5	3040 ± 140	11.52	2963	-405	543
39	NGC 2312	7.6	0.33 ± 0.01	0.16 ± 0.05	0.15	11.9	2245 ± 103	10.58	2030	-928	246
40	NGC 2318	20.0	0.05 ± 0.00	0.65 ± 0.05	0.65	11.2	1335 ± 62	9.48	924	-958	-104
41	NGC 2348	10.0	1.8 ± 0.07	0.13 ± 0.05	0.12	10.2	1070 ± 48	8.42	-139	-969	-432
42	NGC 2331	14.0	1.7 ± 0.12	0.06 ± 0.02	0.06	10.6	1285 ± 59	9.77	1222	-210	337
43	NGC 2338	7.0	0.55 ± 0.02	0.48 ± 0.05	0.47	11.7	1800 ± 83	9.95	1381	-1154	32
44	NGC 2349	18.0	0.75 ± 0.03	0.61 ± 0.10	0.59	11.6	1628 ± 75	9.76	1195	-1106	10
45	NGC 2352	6.0	0.12 ± 0.00	0.32 ± 0.15	0.31	11.5	1750 ± 81	9.57	953	-1455	-191

Table 3. — Continued

Index	Cluster	Diam. <i>arcmin</i>	Age <i>Gyr</i>	E_{B-V} <i>mag</i>	Sch. <i>mag</i>	m-M <i>mag</i>	Dist. <i>pc</i>	R_{gc} <i>kpc</i>	X_{\odot} <i>pc</i>	Y_{\odot} <i>pc</i>	Z_{\odot} <i>pc</i>
46	NGC 2351	10.0	0.24 ± 0.01	0.92 ± 0.25	0.94	12.2	1882 ± 87	9.93	1336	-1325	2
47	NGC 2364	13.0	0.2 ± 0.01	0.31 ± 0.05	0.32	11.7	1919 ± 88	10.00	1401	-1307	101
48	NGC 2408	28.0	3.0 ± 0.12	0.03 ± 0.02	0.03	10.3	1133 ± 52	9.44	794	585	557
49	NGC 2455	8.0	0.18 ± 0.01	0.54 ± 0.10	0.56	12.6	2650 ± 122	10.14	1389	-2254	107
50	NGC 2459	5.4	1.6 ± 0.11	0.03 ± 0.01	0.02	10.6	1300 ± 60	9.64	1060	-640	397
51	NGC 2588 ^c	2.2	0.45 ± 0.01	0.45 ± 0.10	0.45	13.6	4365 ± 201	10.67	1327	-4154	186
52	NGC 2587	4.0	0.1 ± 0.00	0.23 ± 0.10	0.24	11.4	1740 ± 80	9.26	609	-1624	136
53	NGC 2609	5.0	0.8 ± 0.03	0.23 ± 0.10	0.22	10.8	1320 ± 61	8.46	-138	-1280	-291
54	NGC 2666	11.0	3.2 ± 0.13	0.03 ± 0.01	0.03	9.70	860 ± 40	9.36	664	47	544
55	NGC 2678	13.0	2.3 ± 0.09	0.03 ± 0.01	0.03	9.80	900 ± 41	9.24	621	-452	469
56	NGC 2932	21.0	0.5 ± 0.02	0.55 ± 0.10	0.56	11.4	1525 ± 70	8.59	-47	-1521	103
57	NGC 2995	7.0	0.05 ± 0.00	1.94 ± 0.30	1.94	9.60	380 ± 17	8.46	-53	-376	-8
58	NGC 3231	7.0	1.4 ± 0.06	0.02 ± 0.02	0.02	9.30	715 ± 33	9.07	401	314	502
59	NGC 3446	15.0	1.0 ± 0.04	0.16 ± 0.05	0.15	11.0	1485 ± 68	8.32	-298	-1417	329
60	NGC 3496 ^c	10.0	0.35 ± 0.01	0.48 ± 0.15	2.43 †	11.5	1640 ± 75	8.10	-548	-1546	-12
61	NGC 3520	3.0	3.2 ± 0.13	0.03 ± 0.01	0.04	10.5	1245 ± 57	8.57	-13	-978	771
62	NGC 3909	16.0	2.0 ± 0.08	0.13 ± 0.05	0.12	10.3	1100 ± 50	8.14	-409	-989	254
63	NGC 4230	10.0	1.7 ± 0.12	0.23 ± 0.10	0.24	11.0	1445 ± 67	7.92	-673	-1265	187
64	NGC 5155	17.0	1.5 ± 0.18	0.06 ± 0.02	2.61 †	$10.2 \pm 0.1 \downarrow$	1070 ± 49	7.9	-647	-852	-16
65	NGC 5269	3.0	0.16 ± 0.11	0.52 ± 0.10	9.13 †	11.2	1410 ± 65	7.69	-886	-1096	-16
66	NGC 5299	33.0	2.0 ± 0.08	0.19 ± 0.05	1.94 †	10.4	1111 ± 50	7.83	-717	-847	40
67	NGC 5381	11.0	1.6 ± 0.11	0.06 ± 0.02	1.60 †	10.4	1170 ± 54	7.77	-776	-874	43
68	NGC 5800	12.0	0.9 ± 0.04	0.62 ± 0.10	0.61	12.2	2146 ± 99	6.92	-1692	-1301	222
69	NGC 5925	24.0	0.25 ± 0.01	0.58 ± 0.10	2.75 †	10.6	1040 ± 48	7.68	-845	-606	31
70	NGC 5998	9.0	2.2 ± 0.09	0.16 ± 0.05	0.15	10.1	981 ± 45	7.56	-886	-257	332
71	NGC 6005 ^c	6.0	1.0 ± 0.04	0.45 ± 0.20	0.84	12.3	2400 ± 110	6.65	-1982	-1348	-125
72	NGC 6334	31.0	0.5 ± 0.02	1.06 ± 0.25	27.11 †	11.0	1025 ± 47	7.49	-1013	-158	8
73	NGC 6360	5.0	0.02 ± 0.00	1.11 ± 0.20	1.10	11.6	1337 ± 62	7.17	-1333	-76	73
74	NGC 6357	5.0	0.4 ± 0.02	1.35 ± 0.30	52.66 †	11.6	1205 ± 55	7.3	-1196	-143	19
75	NGC 6374	3.6	1.3 ± 0.05	0.48 ± 0.05	12.65 †	10.2	900 ± 41	7.6	-897	-73	7
76	NGC 6421	8.0	0.17 ± 0.01	1.26 ± 0.20	1.27	12.0	1505 ± 69	7.0	-1500	-107	-63
77	NGC 6437	15.0	0.2 ± 0.01	0.71 ± 0.05	0.70	10.5	943 ± 43	7.56	-936	-91	-69
78	NGC 6451 ^c	7.2	0.14 ± 0.01	0.71 ± 0.05	1.52 †	12.2	2060 ± 95	6.44	-2059	-19	-58
79	NGC 6525	13.0	2.0 ± 0.08	0.14 ± 0.03	0.14	10.9	1436 ± 66	7.46	-1097	838	393
80	NGC 6573	1.8	0.01 ± 0.00	2.48 ± 0.20	2.53	10.5	460 ± 21	8.05	-454	72	-17
81	NGC 6595	4.0	0.45 ± 0.02	0.94 ± 0.10	11.86 †	11.9	1640 ± 76	6.90	-1607	325	-49
82	NGC 6605	17.0	0.6 ± 0.02	0.52 ± 0.10	7.99 †	10.2	889 ± 40	7.65	-855	244	5
83	NGC 6603 ^c	6.6	0.20 ± 0.08	0.77 ± 0.10	3.43 †	13.4	3495 ± 160	5.15	-3406	778	-80
84	NGC 6588	5.0	1.6 ± 0.11	0.10 ± 0.03	0.08	10.0	960 ± 44	7.68	-783	-437	-342
85	NGC 6659	14.0	4.0 ± 0.16	0.10 ± 0.03	0.11	10.4	1155 ± 53	7.85	-682	888	282
86	NGC 6698	11.0	1.9 ± 0.07	0.32 ± 0.05	0.31	10.59	1150 ± 53	7.37	-1115	182	-215
87	NGC 6724	6.0	0.9 ± 0.03	1.00 ± 0.10	1.00	11.1	1105 ± 51	7.73	-809	750	69
88	NGC 6735	12.0	0.5 ± 0.02	0.87 ± 0.15	1.66 †	11.6	1466 ± 68	7.34	-1209	828	-47
89	NGC 6743	7.0	1.4 ± 0.05	0.19 ± 0.05	0.18	10.4	1111 ± 51	8.01	-539	948	211
90	NGC 6755 ^c	12.8	0.05 ± 0.00	0.84 ± 0.10	2.19 †	12.0	1785 ± 82	7.19	-1394	1113	-52
91	NGC 6773	8.6	0.1 ± 0.00	1.16 ± 0.20	1.24	12.7	2160 ± 100	6.98	-1653	1386	-113
92	NGC 6775	2.4	0.9 ± 0.03	0.48 ± 0.05	0.49	10.8	1185 ± 55	7.58	-947	705	-108
93	NGC 6795	8.0	0.95 ± 0.04	0.45 ± 0.05	0.45	11.0	1320 ± 61	7.54	-1004	845	-141
94	NGC 6815	30.0	0.15 ± 0.01	1.10 ± 0.20	1.83 †	12.5	2024 ± 93	7.76	-945	1788	72
95	NGC 6832	24.0	3.0 ± 0.12	0.10 ± 0.02	0.09	11.3	1750 ± 81	8.74	59	1678	493

Table 3. — Continued

Index	Cluster	Diam. <i>arcmin</i>	Age <i>Gyr</i>	E_{B-V} <i>mag</i>	Sch. <i>mag</i>	m-M <i>mag</i>	Dist. <i>pc</i>	R_{gc} <i>kpc</i>	X_{\odot} <i>pc</i>	Y_{\odot} <i>pc</i>	Z_{\odot} <i>pc</i>
96	NGC 6837	4.6	1.0 ± 0.04	0.25 ± 0.02	0.25	10.1	943 ± 43	7.93	-594	721	-131
97	NGC 6839	6.0	1.4 ± 0.05	0.29 ± 0.05	0.29	11.0	1410 ± 65	7.8	-783	1166	-127
98	NGC 6840	6.0	1.3 ± 0.04	0.25 ± 0.05	0.27	11.7	1970 ± 90	7.42	-1223	1518	-283
99	NGC 6843	5.0	1.3 ± 0.04	0.30 ± 0.05	0.29	11.7	1945 ± 90	7.44	-1203	1501	-284
100	NGC 6846	4.8	0.55 ± 0.02	0.68 ± 0.05	2.07 †	11.4	1445 ± 67	8.09	-525	1345	48
101	NGC 6847	20.0	0.5 ± 0.02	0.58 ± 0.05	3.09 †	11.9	1894 ± 87	7.95	-743	1742	26
102	NGC 6856	3.2	1.8 ± 0.06	0.16 ± 0.02	0.15	11.3	1704 ± 79	8.66	-9	1657	398
103	NGC 6858	10.0	2.5 ± 0.10	0.13 ± 0.02	0.14	10.7	1310 ± 60	7.75	-805	1007	-234
104	NGC 6859	10.0	3.0 ± 0.12	0.19 ± 0.05	0.18	10.8	1335 ± 62	7.56	-957	856	-364
105	NGC 6871 ^c	32.0	0.01 ± 0.00	0.45 ± 0.05	2.01 †	11.4	1585 ± 73	8.17	-472	1512	57
106	NGC 6873	15.0	0.88 ± 0.04	0.35 ± 0.05	0.36	10.8	1250 ± 58	7.96	-613	1081	-134
107	NGC 6895	16.0	1.0 ± 0.04	0.35 ± 0.05	0.34	10.6	1141 ± 53	8.5	-81	1126	164
108	NGC 6904	8.0	1.0 ± 0.04	0.39 ± 0.05	0.40	11.0	1355 ± 62	8.05	-545	1232	-149
109	NGC 6938	7.2	1.3 ± 0.04	0.13 ± 0.05	0.12	10.6	1250 ± 58	8.05	-521	1112	-233
110	NGC 6950	15.0	1.8 ± 0.05	0.06 ± 0.02	0.08	10.2	1070 ± 49	8.04	-499	904	-281
111	NGC 7023	14.4	0.12 ± 0.00	1.10 ± 0.10	12.02 †	9.70	560 ± 26	8.65	132	527	137
112	NGC 7011	4.4	0.4 ± 0.01	1.08 ± 0.10	3.17 †	11.4	1236 ± 57	8.55	-40	1235	13
113	NGC 7005	4.0	2.5 ± 0.10	0.03 ± 0.01	0.04	10.1	1033 ± 48	7.69	-689	497	-588
114	NGC 7024	5.0	0.5 ± 0.02	1.10 ± 0.10	1.06	12.2	1760 ± 81	8.51	-175	1747	-119
115	NGC 7039 ^c	11.6	0.075 ± 0.00	0.13 ± 0.05	0.87	10.0	950 ± 44	8.52	-35	949	-28
116	NGC 7037	6.0	2.1 ± 0.08	0.16 ± 0.05	0.15	11.0	1485 ± 68	8.35	-276	1437	-252
117	NGC 7050	7.0	2.0 ± 0.08	0.16 ± 0.05	0.16	10.5	1179 ± 54	8.41	-171	1152	-180
118	NGC 7055	5.0	0.8 ± 0.03	1.10 ± 0.10	1.10	11.5	1275 ± 59	8.76	165	1258	124
119	NGC 7071	8.0	0.3 ± 0.01	1.14 ± 0.20	1.12	12.1	1684 ± 78	8.71	42	1682	-59
120	NGC 7084	16.0	1.5 ± 0.06	0.10 ± 0.05	0.11	9.50	765 ± 35	8.27	-239	655	-315
121	NGC 7093	13.0	0.9 ± 0.04	0.61 ± 0.05	0.58	11.8	1785 ± 82	8.72	32	1780	-135
122	NGC 7129	7.0	0.12 ± 0.01	0.97 ± 0.05	7.01 †	11.0	1070 ± 49	8.84	280	1016	184
123	NGC 7127	5.0	0.4 ± 0.02	0.90 ± 0.05	2.17 †	11.6	1445 ± 67	8.82	199	1431	29
124	NGC 7134	3.0	3.3 ± 0.13	0.06 ± 0.02	0.05	10.2	1065 ± 49	7.74	-558	502	-755
125	NGC 7175	32.0	0.25 ± 0.01	0.87 ± 0.05	1.72 †	12.2	1930 ± 89	9.03	326	1902	-3
126	NGC 7193	13.0	4.5 ± 0.18	0.03 ± 0.01	0.05	10.2	1080 ± 50	8.2	-304	839	-608
127	NGC 7352	9.0	0.05 ± 0.00	1.10 ± 0.20	1.08	13.0	2550 ± 117	9.52	698	2452	-47
128	NGC 7380 ^c	13.0	0.014 ± 0.00	0.61 ± 0.05	9.43 †	12.2	2145 ± 99	9.36	632	2049	-33
129	NGC 7394	9.0	0.6 ± 0.02	0.35 ± 0.05	0.34	10.9	1310 ± 60	8.92	332	1259	-147
130	NGC 7429	14.0	0.04 ± 0.00	1.16 ± 0.10	2.34 †	11.4	1190 ± 55	8.96	387	1125	6
131	NGC 7686	16.0	2.0 ± 0.08	0.20 ± 0.05	0.19	11.1	1534 ± 71	9.13	502	1416	-307
132	NGC 7708	24.0	2.0 ± 0.08	0.42 ± 0.05	0.43	11.4	1607 ± 74	9.35	726	1401	301
133	NGC 7795	21.0	0.45 ± 0.02	1.00 ± 0.10	1.03	12.5	2105 ± 97	9.62	935	1885	-79

^c Calibrated clusters, which are listed in Table 2.

† Unreliable/Overestimated reddening values.